

Field distribution and flux-line depinning in the mixed-state of MgB₂ probed by Conduction Electron Spin Resonance

R.R. Urbano,¹ P.G. Pagliuso,¹ C. Rettori,¹ Y. Kopelevich,¹ N.O. Moreno,² and J.L. Sarrao²

¹*Instituto de Física "Gleb Wataghin" UNICAMP, 13083-970
Campinas, SP, Brazil.*

²*Los Alamos National Laboratory, Los Alamos, New Mexico 87545, U.S.A.
(November 17, 2018)*

We report the first observation of the internal magnetic-field distribution and flux-line *depinning* in the vortex-state of a type-II superconductor probed by conduction electrons spin resonance (CESR) technique. The CESR measurements were performed in the recently discovered MgB₂ type-II superconductor compound with transition temperature $T_c \simeq 39$ K using microwave sources at 4.1 (S-band) and 9.5 GHz (X-band) corresponding to resonance fields of $H_r \simeq 1455$ and 3390 Oe for $g \simeq 2.00$ in the normal state, respectively. From the distortion of the CESR line in the superconducting state, the field distribution function, $n(H)$, in the vortex-state was inferred, and from the broadening of the line a direct estimate of the standard deviation, $\sigma \sim 14$ Oe, was obtained at ≈ 28 K and ≈ 7 K for S-band and X-band, respectively. Furthermore, our experiments allowed the determination of the flux-line lattice *depinning* temperature for both employed microwave frequencies.

76.30.Pk,71.30.+h,71.27.+a

In the early 70's almost simultaneously three groups reported the observation of electron spin resonance (ESR) of localized magnetic impurities in the mixed-state of type-II intermetallic superconductors. [1–3] The effects caused by the superconducting state on the resonance lineshape, field for resonance (g -value), and resonance linewidth were later discussed in detail by Davidov *et al.* [4] Concurrently, Orbach [5] showed that the gross observed features could be explained in terms of the internal magnetic-field distribution in the Abrikosov vortex-lattice. [6] Following the Lasher's calculations using the Ginzburg-Landau equations [7] and the analysis of the nuclear magnetic resonance (NMR) data in Vanadium given by Fite and Redfield, [8,9] Orbach was able to simulate most of the observed features based on the Abrikosov vortex-lattice internal magnetic-field distribution of a type-II superconductor. Although CESR experiments in normal metals were discovered in the early 50's, [10] only in the 80's Vier and Schultz reported the first observation of CESR in the superconducting mixed-state of the Nb type-II superconductor. [11] However, due to the low H_{c2} [$H_{c2}(T = 0) \approx 4$ kOe], strong decrease of the CESR intensity, narrowing effects, relaxation phenomena, and weak pinning in the superconducting state, [12–14] these authors have not observed the effects of the vortex-lattice field distribution in their CESR experiments. Nemes *et al.* [15] reported the observation of the CESR in the superconducting state of K₃C₆₀ [$T_c(H = 0) \approx 19$ K, $H_{c2}(T = 0) \approx 25$ T]. Nonetheless, the observed T -dependence of the CESR linewidth below T_c did not allow them to distinguish between the contribution of the field distribution in the vortex-lattice from that of the relaxation processes. [12–14] More recently, Simon *et al.* [16] reported CESR in MgB₂. However, they have observed the vortex-lattice field distribution

either, probably, due to the high field/frequency used in their experiments.

In this work we report, the first direct and unambiguous observation of the internal magnetic-field distribution and flux-line *depinning* in a type-II superconductor probed by conduction electrons (*ce*). The standard deviation of the field distribution has been quantitatively estimated from the experiment.

The recent discovery of superconductivity in the binary compound MgB₂ at $T_c \simeq 40$ K [17] and its high upper critical field $20 \text{ T} \lesssim H_{c2}^{\parallel, \perp c} \lesssim 30 \text{ T}$ [18] have attracted much interest and stimulated us to investigate the mixed-state of this type-II superconductor by means of CESR. To probe the vortex-lattice internal magnetic-field distribution by *ce* we have chosen our two lowest available microwave sources to perform the CESR experiments. The S-band ($\nu \approx 4.1$ GHz, $H_r \approx 1455$ Oe for $g = 2.00$ in the normal state) and X-band ($\nu \approx 9.5$ GHz, $H_r \approx 3390$ Oe for $g = 2.00$ in the normal state) is well suited for this purpose, since for $T \ll T_c$ the CESR field, H_r , will be above $H_{c1} \lesssim 500$ Oe and well below the irreversibility field, $H_r \ll H_{irr}^{\parallel, \perp c} < H_{c2}^{\parallel, \perp c}$ (see below) and, therefore, the *ce* will be certainly probing the internal magnetic-field distribution in the vortex-lattice. Besides, at $\nu \approx 9.4$ GHz and $T \gtrsim 40$ K the lowest estimates for the skin depth $\delta \gtrsim 1 \mu\text{m}$ [$\delta = \sqrt{\rho/\pi\mu_0\nu}$, and $\rho(T)$ from ref. [20]] is larger than the average size of our fine powder particles (our MgB₂ particle size ranged between $0.5 \mu\text{m}$ and $1 \mu\text{m}$, determined by optical microscopy). These two constrains improve the CESR signal/noise ratio and simplify the analysis of the CESR spectra, since a pure absorption lorentzian line is expected to be observed at all temperatures. [21]

The MgB₂ polycrystalline sample was prepared in

sealed Ta tubes as described previously. [22] X-ray powder diffraction analysis confirmed single-phase purity and AlB_2 -type structure for our MgB_2 sample. The zero field cooled (ZFC) and field cooled cooling (FCC) diamagnetism was measured by dc -magnetization in a SQUID MPMS-QD magnetometer at 10 Oe and at the S and X-band CESR fields of 1455 Oe and 3387 Oe, respectively. The CESR experiments were carried out in an ELEXSYS-CW S and X-band Bruker spectrometer using a flexline probehead line with a dielectric ring/split ring low Q cavity module for S-band and a TE_{102} cavity for X-band. The microwave and external fields were always mutually perpendicular. The microwave power was kept as low as 0.1-0.5 mW to minimize the unpleasant noise induced by the ac -microwave and modulation fields in the superconducting mixed-state and, when necessary, 4 scans were accumulated to improve the signal/noise ratio. A 100 kHz field modulation/lock-in signal detection system and a He gas flux T -controller were used.

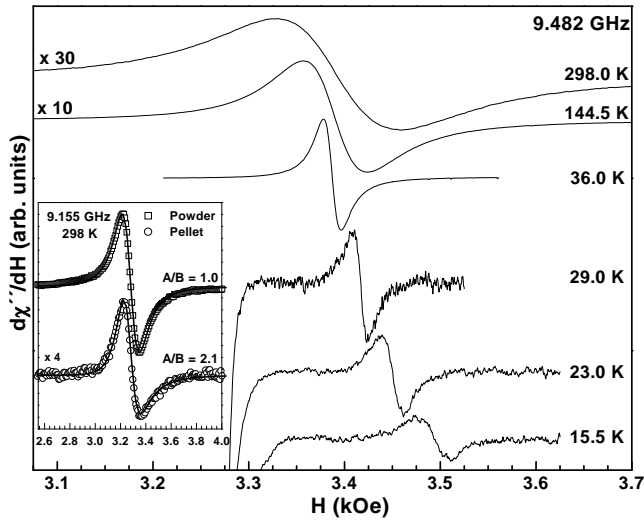


FIG. 1. X-band CESR spectra of MgB_2 at various temperatures above and below $T_c = 39$ K. The inset shows, in open symbols, the X-band CESR spectra at room temperature for a fine powder and a pellet made out pressing the same powder and the solid lines are the fittings to Lorentzian and Dysonian lineshapes.

Figure 1 presents the FCC X-band CESR spectra at few temperatures above and below the transition temperature T_c (3387 Oe) $\simeq 36$ K for a fine powder sample of MgB_2 . Above T_c the lineshape is Lorentzian. Calibration of the CESR intensity against a strong pitch in KCl at room- T leads to $\approx 3.6 \times 10^{20}$ spin/cm³ and a spin susceptibility of $\chi_s \approx 1.4(5) \times 10^{-5}$ emu/mole. Using a free electron gas approximation ($\chi = \mu_B^2 N(0)$) we extracted the density of states (DOS) at the Fermi level, $N(0) \approx 0.42(5)$ states/eV-unit cell, which is of the order of that obtained from a band structure calculation. [23] The inset of Fig. 1 shows the X-band CESR spec-

tra measured at room temperature for a fine powder and for a pellet made out of the same powder. For the pellet sample we observed a CESR of Dysonian lineshape with $A/B \approx 2.1$ (admixture of absorption and dispersion of Lorentzian line) indicating a sample size larger than or comparable with the skin depth, δ , [21] and with an intensity smaller than that in the fine powder. These results confirm that the CESR indeed comes from the bulk of the sample under study. We want to point out that in all our experiments a single resonance was always observed. FCC and ZFC X-band CESR in the superconducting mixed-state at 19.3 K for the same sample of Figure 1 are shown in Fig. 2a. It is clear from these measurements that the shift toward higher fields of the CESR, ~ 20 Oe larger for the ZFC experiment, is caused by the diamagnetic shielding effect in the superconducting state. Fig. 2b presents the superconducting transition measured for this sample by dc -magnetic susceptibility, $\chi_{dc}(T)$, in a ZFC and FCC experiments at 10 Oe, 1455 Oe (S-band), and 3387 Oe (X-band). The inset of Fig. 2b shows, for the three applied fields, the onset of superconductivity, $T_c(H)$, and the irreversibility points, $T_{irr}(H)$. For $H = 10$ Oe we obtained $T_c \simeq T_{irr} = 39$ K.

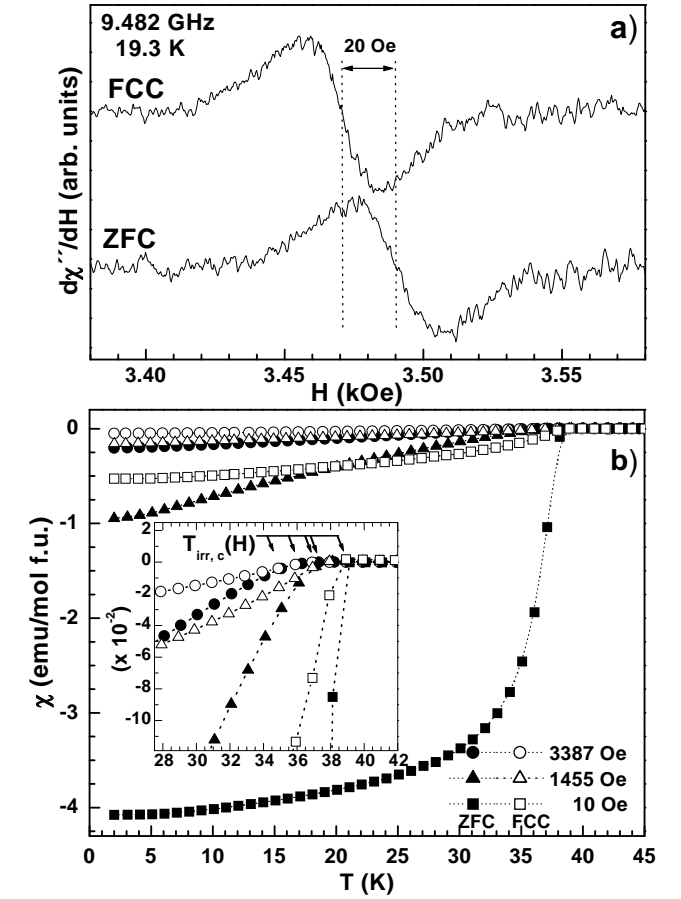


FIG. 2. a) FCC and ZFC X-band CESR spectra at 19.3 K, b) T -dependence of the FCC and ZFC dc -magnetic susceptibility of MgB_2 for $H = 10$ Oe, 1455 Oe and 3387 Oe.

Regarding the normal state properties of MgB₂, we found, for $T \gtrsim 200$ K and a Pauli-like T -independent magnetic susceptibility $\chi_{dc}(T) = 2.5 \times 10^{-5}$ emu/mole, after taking into account the core diamagnetism. Comparing this value with that obtained from the DOS calculated theoretically, $N(0) \approx 0.65(5)$ states/eV·unit cell and using $\chi = \mu_B^2 N(0)$, one can estimate the Stoner's factor $\chi_{dc}/\chi = 1/(1 - \alpha) \approx 1.19$ ($\alpha \approx 0.16(6)$) due to the electron-electron exchange interactions in MgB₂. Estimates of χ using the Sommerfeld constant $\gamma = 1/3\pi^2 k_B^2 N(0)(1 + \lambda) \approx 2.6$ mJ/mole K², [24,25] are not reliable due to the large uncertainty found in the literature for the value of the electron-phonon coupling, λ . [19,26–28]

Below we discuss the CESR results obtained in a FCC experiments. The T -dependence of the relative intensity, $I(T)/I^n(40\text{ K})$, the shift of the field for resonance relative to that in the normal state, $H_r(T) - H_r^n(40\text{ K})$, and the linewidth, $\Delta H_{pp}(T)$ of the CESR measured at X and S-bands, are presented in Figs. 3a, b, and c, respectively, for the sample of Fig. 1. In the normal state, $T \gtrsim 39$ K, we found that the CESR lineshape is lorentzian at all T and, within the accuracy of the measurements, $I^n(T)$ and $H_r^n(T)$ are T -independent indicating that the resonance can be attributed to itinerant ce ($g = 2.003(2)$) as expected for a light metal. [30] Fig. 3c shows that above ~ 33 K the linewidth, ΔH_{pp} , is frequency independent suggesting homogeneous CESR. Between 40 K and 110 K ΔH_{pp} follows roughly the T -dependence of the resistivity, $\rho(T)$, exemplified by the data reported by Canfield *et al.* for a MgB₂ wire. [20] This result suggests that in this temperature region the ce spin-lattice relaxation is dominated by phonons via spin-orbit coupling. [29,30] However, above 110 K a clear departure of $\Delta H_{pp}(T)$ from $\rho(T)$ is observed, and above ~ 250 K the linewidth levels off at about 130 Oe. This is an intriguing result because it shows that while the ce mean-free path is still decreasing at high- T the spin-flip scattering remains about the same.

In the superconducting state, $T \lesssim 39$ K, the CESR data in both bands present the following features: *i*) a strong drop of the CESR signal/noise ratio becoming almost undetectable at ~ 4.2 K ($T/T_c \approx 0.1$) in X-band (see Fig. 3a), *ii*) an evident resonance shift toward higher fields (see Fig. 3b and inset), *iii*) the linewidth, ΔH_{pp}^s , does not change down to ~ 35 K and ~ 26 K for S and X-band, respectively, keeping approximately the same value as in the low- T normal state, $\Delta H_{pp}^n \approx 18$ Oe (see Fig. 3c), and *iv*) a broadening and distortion of the line (with larger broadening toward the low field side of the resonance) is observed below ~ 35 K and ~ 26 K for S and X-band, respectively. The drop of $I(T)/I^n(40\text{ K})$ for $T \lesssim 39$ K is attributed to the decreasing of normal ce excited across the superconducting gap, Δ ($1.8 \div 3$ meV). [33] The fraction of normal ce at $T \approx 7$ K, $I(7\text{ K})/I^n(40\text{ K}) \approx 0.7$, is relatively large, which is a consequence of the mixed-state in type-II superconductors. The increase of $H_r(T)$ for $T \lesssim 35$ K in Fig. 3b is caused by the partial

shielding of the external field by the supercurrents (see also Fig. 1). Below ~ 50 K the linewidth, ΔH_{pp} , is the same in both bands and remains constant at $\approx 18(2)$ Oe down to 35 K and 26 K for S and X-bands, respectively, (see Figs. 3c and 4b).

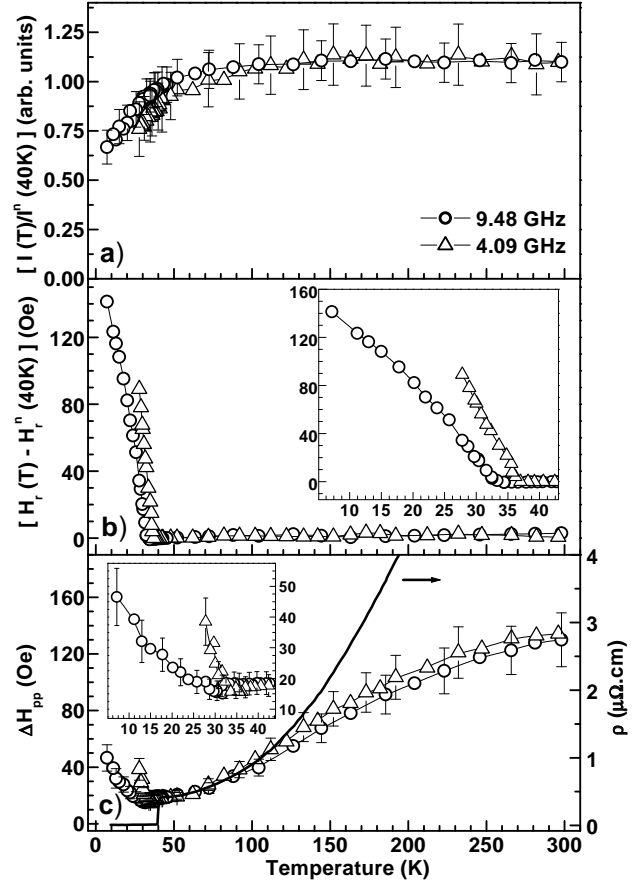


FIG. 3. X and S-band T -dependence of the: a) relative CESR intensity, $I(T)/I^n(40\text{ K})$, b) shift of the resonance field, $H_r(T) - H_r^n(40\text{ K})$, and c) linewidth, $\Delta H_{pp}(T)$, and resistivity, $\rho(T)$, from ref. [20].

Besides, in these T -intervals, as in the normal state, the lineshape remains lorentzian. These results suggest that: a) for the S and X-bands, the corresponding temperature intervals $35 \lesssim T \lesssim 37$ K and $26 \lesssim T \lesssim 35$ K may be associated with a vortex-*viscous* motion regime that, via a motional narrowing mechanism, may be responsible for the absence of the inhomogeneous line broadening expected from the magnetic-field distribution in a vortex-pinned lattice, and b) the ce relaxation in the superconducting state of MgB₂ was found to be T -independent, except for a tiny decrease of ΔH_{pp}^s (smaller than our error bars, see Fig. 3c).

However, below ~ 35 K and ~ 26 K for the S and X-band, respectively, the CESR line clearly broadens and distorts revealing the presence of a field distribution that we now attribute to a vortex-*pinning* regime. It is worth

mention that this broadening cannot be attributed to a random distribution of the anisotropic upper critical field, $H_{c2}^{\parallel, \perp c}$, because at the temperature where the S-band CESR starts broad the X-band linewidth remains narrow (see Fig. 3c).

The spectra shown in Fig. 4a are the X-band CESR at ~ 15.5 K and ~ 23.0 K. The observed lineshapes present the general features expected for the CESR absorption derivative of ce probing the internal magnetic-field distribution in a vortex-lattice of a type-II superconductor. Notice that the signal/noise ratio is much smaller than that in the normal state due to a decreasing number of normal ce in the superconducting state (see above) and the inevitable noise produced by the interaction between vortices and the external microwave and modulation ac -fields needed for the detection of the CESR. [31]

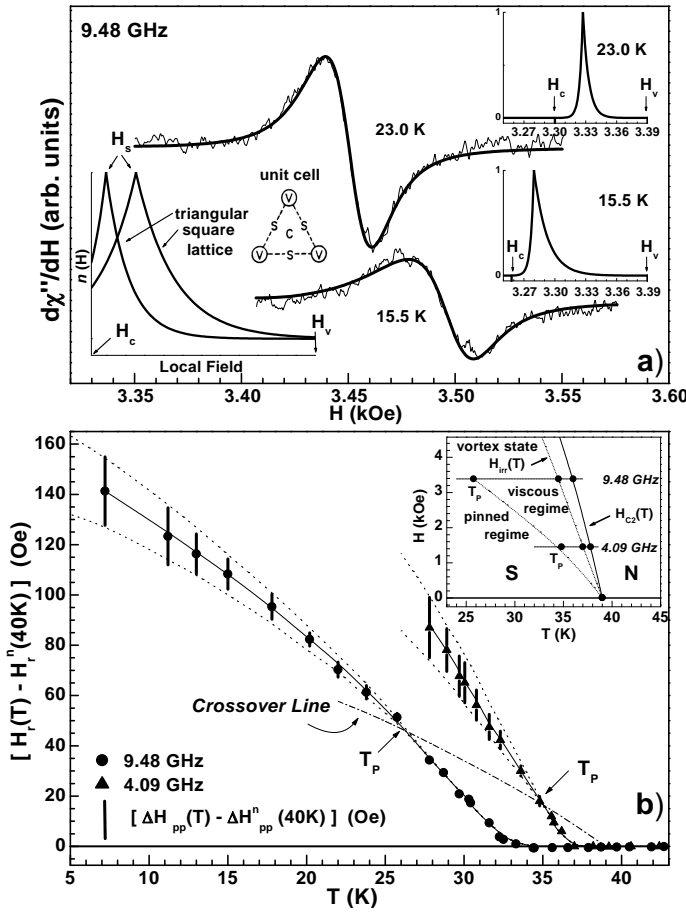


FIG. 4. a) X-band CESR spectra at 15.5 K and 23.0 K. Left-bottom inset: triangular unit cell and Lasher's NMR lineshape, $n(H)$, for triangular and square vortex-lattices. Solid lines in a) are simulations obtained by the convolution of a lorentzian absorption line of $\Delta H_{pp}^n(40 \text{ K}) = 18 \text{ Oe}$ and $H_r^n(40 \text{ K}) = 3390 \text{ Oe}$ with a Lasher-like distribution. The best distributions, $n(H)$, are shown in the right-side insets. b) T -dependence of $H_r(T) - H_r^n(40 \text{ K})$ (closed symbols), and $\Delta H_{pp}(T) - \Delta H_{pp}^n(40 \text{ K})$ (solid bars). Notice that the solid bars are not "error bars". The inset presents the low field superconducting state phase-diagram for MgB_2 . The crossover line separating vortex-pinning and viscous regimes $T_p(H)$ extracted from the CESR data and irreversibility line obtained from the dc -magnetic susceptibility data (see Fig. 2) are shown.

The left-bottom inset of Fig. 4a shows the theoretical NMR absorption lineshape, $n(H)$, calculated by Lasher, using Ginzburg-Landau equations, [7] due to the internal magnetic-field distribution in a triangular ($(H_S - H_C)/(H_V - H_C) \approx 7\%$) and square ($(H_S - H_C)/(H_V - H_C) \approx 20\%$) Abrikosov vortex-lattice, where the points in space correspond to the maximum, H_V , minimum, H_C , and saddle, H_S (majority lattice points) fields in the unit cell of a triangular lattice. For simplicity we have assumed an Abrikosov vortex-lattice and calculated the derivative of the convolution of a NMR Lasher-like absorption lineshape, $n(H)$, with an absorption derivative in the superconducting state. In this simulation we have considered: *i*) for the maximum field, H_V , the value of the resonance field in the normal state, $H_r^n \approx 3390 \text{ Oe}$, *ii*) a linewidth, $\Delta H_{pp}^s \approx \Delta H_{pp}^n(40 \text{ K}) \approx 18(2) \text{ Oe}$ (no relaxation contributions were contemplated [12–14]), and *iii*) two adjustable parameters, H_S and H_C ($< H_S < H_V$) (notice that CESR is an experiment at fixed frequency, therefore, the diamagnetic shift of the line will be always toward higher fields). The results of these convolutions are given in Fig. 4a by the solid lines on the observed spectra. The reasonable agreement obtained between the data and the simulation indicates that the broadening and distortion of the CESR lines may be accounted for by the magnetic-field distribution in the vortex-lattice state and that relaxation process is not present in the superconducting state of MgB_2 . According to the results presented in the insets of Fig. 4a the field distribution deviates from that expected for ideal either triangular or square vortex-lattice. We attribute this fact to the vortex-lattice distortions due to the presence of relatively strong vortex pinning effect in our sample.

Figure 4b presents a summary of the most relevant CESR data in the superconducting state of MgB_2 . The closed symbols give the shift of the resonance field in the superconducting state, $H_r(T) - H_r^n(40 \text{ K})$, and the solid bars represent the "extra" broadening of the linewidth

in the superconducting state relative to that in the normal state, $\Delta H_{pp}^s(T) - \Delta H_{pp}^n(40\text{ K})$ (notice that these solid bars are not "error bars"). This "extra" broadening may actually be directly associated to the standard deviation, 2σ , of the field distribution. The temperature where the resonance field, $H_r^s(T)$, departs from $H_r^n(40\text{ K})$ agrees, within $\sim 1\text{ K}$, with the critical temperature, $T_c(H)$, obtained from the onset of superconductivity in Fig. 2b. The temperature where the $\Delta H_{pp}^s(T)$ exceeds that of the normal state $\Delta H_{pp}^n(40\text{ K})$, defines the vortex-pinning temperature, $T_p(H)$. This temperature separates *pinning* and *viscous* vortex motion regime. The microwave field, H_1 , induces a screening current which exerts a force on flux-lines $j\Phi_0$ (j is the current density) per unit length tilting the flux-lines in the direction of H_1 ($H_1 \perp H_r$). This force is balanced by *pinning* and *viscous* forces $\alpha_p x + \eta v = j\Phi_0$, [32] where α_p is the *pinning* constant (Labush parameter), x is the vortex displacement, η is the *viscous* drag coefficient (viscosity), and v is the flux line velocity. So, from the equation of motion one gets the vortex resistivity $\rho_v = (\Phi_0 H / \eta) / (1 + i\omega_0 / \omega)$ [32], where $\omega_0 = \alpha_p / \eta$, the so-called *depinning* (crossover) frequency, separates the *pinning* ($\omega \ll \omega_0$) and *viscous* flux flow ($\omega \gg \omega_0$) regimes. We estimate the in-plane viscosity coefficient $\eta = \Phi_0 H_{c2}^{\parallel c} / \rho_n \approx 10^{-6}\text{ N s/m}^2$, taking $H_{c2}^{\parallel c} = 2\text{ T}$ [16] and $\rho_n = 0.4\ \mu\Omega\text{ cm}$ [20]. From low- T ($T = 6\text{ K}$) magnetization hysteresis loop $M(H)$ measurements and using the Bean critical state model applied to a disk-shaped sample, we estimate the critical current density $j_c(T = 6\text{ K}, H = H_r = 3535\text{ Oe}) \approx 10^{11}\text{ A/m}^2$ being in a good agreement with previous results [33]. From the equation for the *pinning* force $f_p = j_c \Phi_0 = \alpha_p \xi$ ($\xi = \sqrt{\Phi_0 / 2\pi H_{c2}^{\parallel c}}$ is the in-plane coherence length [32]) we estimate $\alpha_p \approx 1.5 \times 10^4\text{ N/m}^2$, and finally $\omega_0 \approx 1.5 \times 10^{10}\text{ rad/s}$ ($\nu_0 = \omega_0 / 2\pi \approx 2\text{ GHz}$). Because the obtained value of ν_0 is comparable to the measuring frequency, $\nu = 9.4\text{ GHz}$, and $j_c(T)$ decreases with T , it is reasonable to assume the vortex "depinning" occurring at $T \geq T_p(\nu)$ and motional narrowing effects may, then, account for the reduction of $\Delta H_{pp}^s(T)$ toward $\Delta H_{pp}^n(T)$. If such an interpretation is correct, $T_p(\nu)$ should be shifted to higher- T by lowering the measuring frequency. This is actually shown by our experiments at 4.1 GHz (see Fig. 4b). On the other hand, for $\nu \gg \nu_0$ no crossover to the *pinning* regime is expected and, therefore, no "extra" broadening of the line, $\Delta H_{pp}^n(T)$, would be expected below T_c . The measurements performed in Ref. [16] for $\nu \geq 35\text{ GHz}$, which according to our estimation is well above ν_0 , revealed at $T = 5\text{ K}$ a broadening and a splitting of the line that was attributed to the coexistence of CESR in the normal and superconducting state. The dashed line in Fig. 4b is the crossover line which separates *pinning* and *viscous* FLL motion regimes of MgB₂ obtained from our CESR experiments. The inset in Fig. 4b presents a low field phase-diagram for the superconducting state of our MgB₂ sample extracted from CESR

and *dc*-magnetization experiments and summarizes the discussion above.

Finally, it is important to mention that the results presented in this letter and those of Simon *et al.* [16] are somehow complementary, although below T_c none of our spectra showed the CESR corresponding to the normal phase reported in Ref. [16].

In summary, we demonstrate that CESR can be used for direct probing of the inhomogeneous field distribution in the mixed state of the MgB₂. The standard deviation, σ , of the field distribution has been inferred for various temperatures from the "extra" broadening of the linewidth. The obtained σ -value of $\sim 14\text{ Oe}$ at $T \approx 28\text{ K}$ and $T \approx 7\text{ K}$ for S-band and X-band, respectively, is of the order of the values extracted from the analysis of the muon-spin rotation data in high- T_c cuprates. [34] The small value of σ ($0.5 \div 1\%$ of the applied fields) is consistent with the relatively large value of the Ginzburg-Landau parameter $\kappa = \lambda / \xi \sim 10 \div 20$ for MgB₂. [19] Besides, the CESR data has allowed to determine "depinning" temperature $T_p(H, \nu)$ separating vortex-pinning and *viscous* vortex motion regimes.

The authors are grateful to Prof. O.F. de Lima for critically reading of the manuscript. This work was supported by FAPESP and CNPq of Brazil.

-
- [1] C. Rettori, D. Davidov, P. Chaiken, and R. Orbach, Phys. Rev. Lett. **30**, 437 (1973).
 - [2] U. Engel, K. Baberschke, G. Koopman, S. Hufner, and M. Wilhem, Solid State Commun. **12**, 977 (1973).
 - [3] H.E. Alekseevski, I.A. Garifullin, B.I. Kochelaev, and E.G. Kharakhashyan, JETP **18**, 323 (1973).
 - [4] D. Davidov, C. Rettori, and H.M. Kim, Phys. Rev. **B9**, 147 (1974).
 - [5] R. Orbach, Phys. Letters **47A**, 281 (1974).
 - [6] A.A. Abrikosov, Soviet Phys. JETP **5**, 1174 (1957).
 - [7] G. Lasher, quoted in ref. [9]
 - [8] W. Fite and A.G. Redfield, Phys. Rev. **162**, 358 (1962).
 - [9] A.G. Redfield, Phys. Rev. **162**, 367 (1962); W. Fite and A.G. Redfield, Phys. Rev. Lett. **17**, 381 (1966).
 - [10] T.W. Griswold, A.F. Kip, and C. Kittel, Phys. Rev. **88**, 88 (1952).
 - [11] D.C. Vier and S. Schultz, Phys. Letters **98A**, 283 (1983).
 - [12] K. Maki, Phys. Rev. **B8**, 191 (1973).
 - [13] C. Tsallis, Phys. Stat. Sol. **79**, 451 (1977).
 - [14] Y. Yafet, Phys. Letters **98A**, 287 (1983).
 - [15] N.M. Nemes, J.E. Fischer, G. Baumgartner, L. Forró, T. Fehér, G. Oszlányi, F. Simon, and A. Lánossy, Phys. Rev. **B61**, 7118 (2000).
 - [16] F. Simon, et. al., Phys. Rev. Lett. **87**, 047002-1 (2001).
 - [17] J. Nagamitsu, N. Nagakawa, T. Muranaka, Y. Zenitani, and J. Akimitsu, Nature **410**, 63 (2001).
 - [18] O.F. Lima, R. A. Ribeiro, M.A. Avila, C.A. Cardoso and A.A. Coelho, Phys. Rev. Lett. **86**, 5974 (2001).

- [19] S. Patnaik et. al., Superconductors, Science & Technology, Vol. **14**, No. 6 (June 2001) R315.
- [20] P. C. Canfield, D.K. Finnemore, S. L. Bud'ko, J.E. Ostenson, G. Lapertot, C. E. Cunningham, C. Petrovic, Phys. Rev. Lett. **86**, 2423 (2001).
- [21] F.J. Dyson, Phys. Rev. **98**, 349 (1955); G. Feher and A.F. Kip, Phys. Rev. **98**, 337 (1955).
- [22] S.L. Bud'ko, G.Lapertot, C. Petrovic, C.E. Cunningham, N. Anderson, P.C. Canfield, Phys. Rev. Lett. **86**, 1877 (2001).
- [23] J. Kortus, I.I. Mazin, K.D. Belashchenko, V.P. Antropov, and L.L. Boyer, Phys. Rev. Lett. **86**, 4656 (2001).
- [24] F. Bouquet, R.A. Fisher, N.E. Phillips, D.G. Hinks, and J.D. Jorgensen, Phys. Rev. Lett. **87**, 047001-1 (2001).
- [25] Y. Wang, T. Plackowski, and A. Junod, Physica C, Vol. 355, 179 (2001).
- [26] T. Yildirim et al., Phys. Rev. Lett. **87**, 037001 (2001).
- [27] E. Cappelluti, S. Ciuchi, C. Grimaldi, L. Pietronero, and S. Strassler, Phys. Rev. Lett. **88**, 117003 (2002).
- [28] R. Osborn, E.A. Goremychkin, A.I. Kolesnikov, and D.G. Hinks, Phys. Rev. Lett. **88**, 017005 (2001).
- [29] G. Webb, Phys. Rev. **181**, 1127 (1969).
- [30] Y. Yafet, in: Solid State Physics Vol. **14**, Eds. F. Seitz and D. Turnbull (Academic Press, N.Y. 1963).
- [31] A. Janossy and R. Chicault, Physica C **192**, 399 (1992).
- [32] E. H. Brandt, Rep. Prog. Phys., Vol. **58**, 1465 (1995).
- [33] C. Buzea and T. Yamashita, Superconductors, Science & Technology, Vol. **14**, No. 11 (2001) R115.
- [34] E.H. Brandt, Phys. Rev. Lett. **66**, 3213 (1991); J.E. Sonier, Rev. of Modern Phys. **72**, 769 (2000).